Journal of Energetic Materials
Publication details, including instructions for authors and subscription information:
http://www.informaworld.com/smpp/title~content=t713770432

Twin-Screw Extrusion of Nano-Alumina-Based Simulants of Energetic Formulations Involving Gel-Based Binders

S. Ozkan[a]; H. Gevgilili[a]; D. M. Kalyon[a]; J. Kowalczyk[b]; M. Mezger[c]
[a] Stevens Institute of Technology, Hoboken, New Jersey [b] Material Processing and Research, Hackensack, New Jersey [c] U.S. Army TACOM-ARDEC, Armament Systems Process Division, WECAC, Picatinny Arsenal, New Jersey

To cite this Article Ozkan, S. , Gevgilili, H. , Kalyon, D. M. , Kowalczyk, J. and Mezger, M.(2007) 'Twin-Screw Extrusion of Nano-Alumina-Based Simulants of Energetic Formulations Involving Gel-Based Binders', Journal of Energetic Materials, 25: 3, 173 — 201
To link to this Article: DOI: 10.1080/07370650701399320
URL: http://dx.doi.org/10.1080/07370650701399320

Journal of Energetic Materials, 25: 173–201, 2007

ISSN: 0737-0652 print/1545-8822 online
DOI: 10.1080/07370650701399320

Twin-Screw Extrusion of Nano-Alumina–Based Simulants of Energetic Formulations Involving Gel-Based Binders

S. OZKAN
H. GEVGILILI
D. M. KALYON

Stevens Institute of Technology, Hoboken, New Jersey

J. KOWALCZYK

Material Processing and Research, Hackensack, New Jersey

M. MEZGER

U.S. Army TACOM-ARDEC, Armament Systems Process Division, WECAC, Picatinny Arsenal, New Jersey

A 7.5-mm twin-screw extruder was developed specifically for the processing of energetic formulations involving nanoparticles. Prior to extrusion of energetic formulations, simulants of CMC, water, and alumina nanoparticle gels were extruded. Quantitative measures of degree of mixedness (statistics of concentration distributions) were obtained on samples processed with the twin-screw extruder and with conventional processing methods using wide-angle X-ray diffraction (WAXD) and thermo-gravimetric analysis (TGA) and were corroborated with microscopy. Twin-screw extrusion process generated more

Address correspondence to D. M. Kalyon, Stevens Institute of Technology, Castle Point St., Hoboken, NJ 07030. E-mail: dkalyon@stevens.edu

homogeneous mixtures of nanoparticles than conventional (intensive batch) mixing technologies and the use of surfactants further improved the homogeneity. With increasing homogeneity the suspension exhibited lower elasticity and shear viscosity. Overall, the results of this study emphasize the important roles played by the surface properties of rigid particles, the interfacial tension between the particles and the binder, and the rheological behavior of the binder. In the absence of properly selected binder and surfactant(s), the processing of nanoparticles, without agglomeration, is difficult to achieve. This finding may be relevant to the evaluation of past efforts, which have aimed to improve the ultimate properties of energetic formulations by incorporating nanoparticles.

Keywords: dispersion, extrusion, nanocomposites, nanoenergetics, nanoparticles

Introduction and Background

This research and development project was conducted to support the objectives of the Army After Next (AAN) for highly lethal, more energetic, less sensitive explosives for use in smaller, lighter warheads for anti-armor and missile applications and their transition to the Army industrial base. There were two major objectives: the first was to generate the ability to develop formulations the various properties of which can be tested fast and reliably, and the second was to enable the incorporation of nanoparticles into various energetic formulations using relatively small quantities and under scalable and industrially relevant processing conditions.

First, the development of energetic formulations is a challenge and requires mixing and processing of ingredients at multiple scales. Typically at least three different mixing operations, i.e., hand mixing for the smallest scale followed by batch mixing using a pint-size mixer and batch mixing in a gallon-size mixer, which are in turn followed by larger scales of mixing more relevant to manufacturing. Different scales of mixing and types of mixers generate differences in the statistics of the concentration distributions of the ingredients of the energetic formulation and give rise to changes in associated structuring

and burn rate/mechanical properties [1–4]. Generally there is a mismatch in the properties of the energetic formulations going from one scale of mixing to another, especially when nanoparticles are employed as part of formulation development/testing effort. The results could be misleading, possibly generating time delays in development and cost overruns.

Second, the incorporation of nanoparticles into formulations to produce nanocomposites and nanoenergetic materials is also a significant challenge. Some of the special challenges to produce energetic grains using nanometal powders (5–100 nm range) by encapsulating them into various binders including energetic binders include the need to:

- conserve particle size of nanoparticles by preventing the formation of particle clusters.
- select proper wetting agents and binders.
- tailor the process to the rheological behavior of the dispersion.
- work at relatively small processing rates (especially due to the very high cost of some of the newly available nanoparticles).
- generate very small specimens for further testing and validation for the development of new formulations without resorting to hand mixing or batch mixing at low volumes to generate very poorly mixed samples, which cannot be scaled up.

Here a novel twin-screw extrusion processor was developed specifically to represent the smallest industrially relevant twin-screw extruder ever designed and constructed [5–7]. This 7.5-mm co-rotating twin-screw extruder is equipped with various types of safety features, and thus is differentiated from machinery available to civilian industries. It allows for the first time the development of energetic formulations by generating similar structures for different scales of development while retaining fully the ability to be scaled up to any continuous processing scale. A series of projects with inert materials were also carried out with the 7.5-mm twin-screw extruder to test the safety features of this novel continuous processor, along with tests of its

flexibility, limitations, and ease of use. Here the processing of gel bases systems in conjunction with the novel 7.5-mm twin-screw extruder is presented along with the comparisons to the results of conventional intensive batch mixers for benchmarking of the results.

Experimental

Materials

The materials of the investigation were nanoparticles of α-Al_2O_3 and γ-Al_2O_3 compounded into a hydrogel-based binder. The hydrogel binder consists of carboxymethylcellulose (CMC), available from Hercules, incorporated with deionized water. The relevance of this binder stems from the understanding that most of the current energetic formulations involve solvated nitrocellulose (NC) systems, which form a gel and act as the binder. The dispersion of particles, especially nanoparticles, poses difficult-to-overcome challenges when gels are used as the binders. The rheological behavior of the resulting suspensions as well as the quantitative measures of the degree of mixedness, i.e., the statistics of the concentration distributions, were characterized and compared for the batch and twin-screw–extruded suspensions. Specifically, the degree of mixedness analysis carried out using wide-angle X-ray diffraction (WAXD) and thermo-gravimetric analysis (TGA) of the twin-screw–extruded samples were compared and contrasted with the batch-mixed specimens. The scanning and transmission electron microscopy (SEM and TEM) micrographs and optical micrographs were also used to corroborate the findings of the WAXD and TGA analyses.

Nanoparticles. Nanoparticles of γ-Al_2O_3 were received from Inframat Advanced Materials, LLC (Farmington, CT) and are reported to have a particle size of 40 nm. An SEM micrograph of the γ-Al_2O_3 is shown in Fig. 1 and indicates that the particle sizes of γ-Al_2O_3 are in the 10–100 nm range. The γ-Al_2O_3 nanoparticles appear to be nearly spherical in shape. The α-Al_2O_3 nanoparticles were also received from

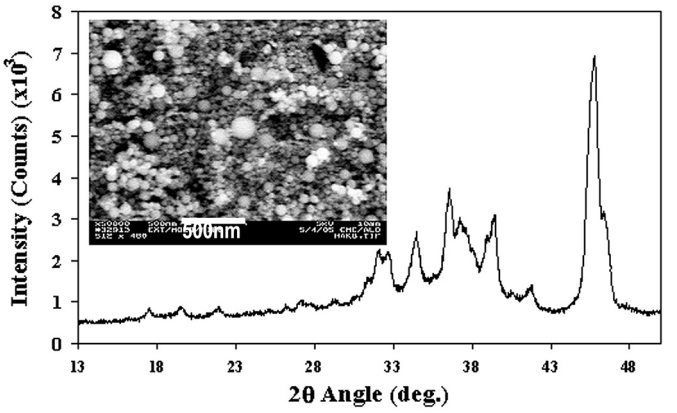

Sample name	Average 2 θ (degree)	Average FWHM	Average crystallite size t (nm)
Pure γ- Al_2O_3	45.746	0.659	13.59

Figure 1. The X-ray diffraction pattern and SEM micrograph of γ-Al_2O_3.

Inframat Avanced Materials, LLC. The reported mean particle size is 150 nm. The SEM micrographs of the α-Al_2O_3 are shown in Fig. 2. The particles exhibit relatively higher aspect ratios in comparison to γ-Al_2O_3 and the particles are flaky. The particle size distribution of the α-Al_2O_3 nanoparticles is broader than that of the γ-Al_2O_3.

The nanoparticles were also subjected to an X-ray analysis to determine their crystallite size using a line-broadening technique. This method determines the mean crystallite size of the particles using the Scherrer analysis. In this X-ray method the full width at half the maximum values of the crystallite peaks associated with α-Al_2O_3 and γ-Al_2O_3 were measured and converted to crystallite sizes. Typical X-ray analysis results for the crystallite sizes of α-Al_2O_3 and γ-Al_2O_3 are shown in Figs. 1 and 2. The Sherrer analysis results from these diffraction patterns indicated that the crystallite sizes of α-Al_2O_3 and γ-Al_2O_3 were 13.6 and 44 nm, respectively (Figs. 1 and 2).

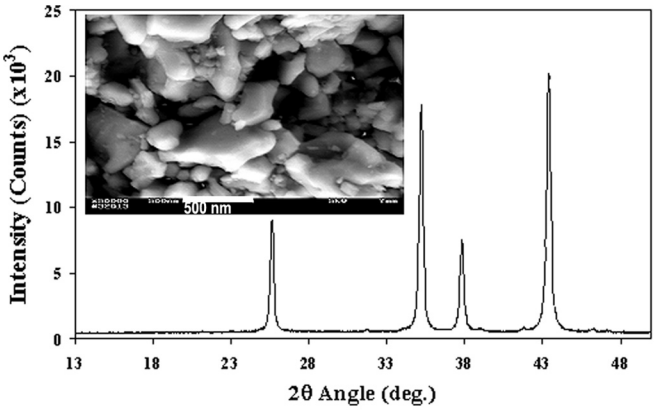

Sample name	Average 2 θ (degree)	Average FWHM	Average crystallite size t (nm)
Pure α- Al_2O_3	46.266	0.262	43.94

Figure 2. The X-ray diffraction pattern and SEM micrograph of α-Al_2O_3.

Binder. The binder of the twin-screw extrusion study was sodium carboxymethylcellulose mixed with deionized (DI) water. The typical linear viscoelastic properties of the hydrogel binder, obtained upon small-amplitude oscillatory shearing, are shown in Fig. 3. The elasticity of the sample is indicated by the storage modulus G', which represents the energy stored as elastic energy during one cycle of deformation. On the other hand, the loss modulus, G'', values are indicative of the energy dissipated as heat during one cycle of deformation. The magnitude of complex viscosity, $|\eta^*|$, approaches the shear viscosity as the shear rate in steady shearing and the frequency in oscillatory shear both approach zero. The strain amplitude sweeps indicated that the CMC hydrogel binder is in the linear viscoelastic range up to a strain amplitude of 4%. On the basis of these strain-dependent scans, the strain amplitude for the characterization of the dynamic properties at different frequencies was selected

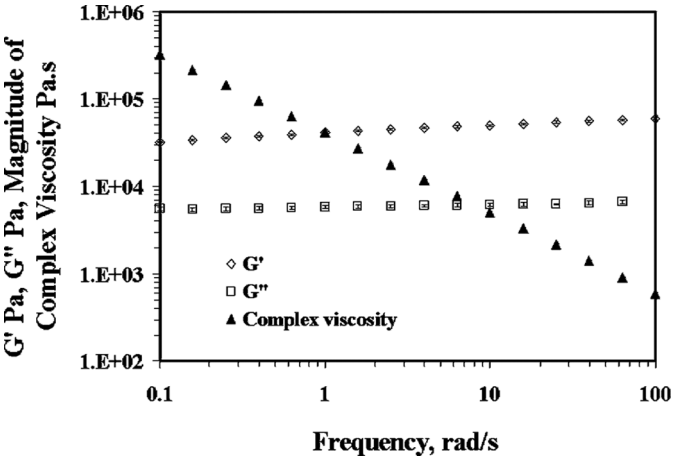

Figure 3. Typical dynamic properties of gel binder.

to be 1%. Time scans were also carried out to determine the duration within which the samples remained stable. The main source of the time dependence was drying of the specimen in the rheometer. The water loss over the course of the 1000-s run was about 2%, which did not appear to significantly affect the rheological properties.

The frequency-dependent dynamic properties of the CMC hydrogel binder are shown in Fig. 3. The hydrogel binder exhibits the typical behavior of a gel with frequency-independent values of the storage, G', and loss moduli, G''. The storage modulus values are about one order of magnitude greater than the loss modulus values, suggesting the relatively high elasticity of the gel network. The higher G' values in comparison to the G'' values are indicative of the solid-like nature of the hydrogel. The parallel nature of the storage and loss modulus values is indicative of the gel structure (see Fig. 3). The gel-like nature of the binder is again indicated by the relatively low and frequency-independent nature of the $\tan \delta = G''/G'$ data. The relatively high elasticity of such gels allows them to be used as process simulants for NC-based systems.

Batch Mixing. An intensive batch mixer/torque rheometer, manufactured by Haake Buchler Instruments, Inc. (Saddle Brook, NJ; EU-5V), with a mixing volume capacity of 60 mL, was used to mix the nanoparticles with the hydrogel binder at a temperature of 25°C. Such intensive mixers are used partially full and a degree of fill of 60% was employed during the batch mixing. The torque, T, and hence the specific energy, E_s, input generated during the mixing process could be monitored during mixing as:

$$E_s = \frac{\Omega \int^{t_m} T dt}{M_t} \quad (1)$$

where Ω is the rotational speed of the blades of the mixer, t is time, M_t is the total weight of the mixture in the mixer, and t_m is the duration of the batch mixing. In the batch mixing experiments, the total duration of the mixing process, t_m, was varied systematically in order to assess the effects of the specific energy input, expanded during the mixing process. Since the addition order of ingredients affects the goodness of mixing, first alumina particles were suspended in DI water and sonicated to stabilize the suspension. Later, CMC polymer was added to this suspension and mixed manually to let the polymer interact with water and form a gel. This premixed paste was then fed into the mixer, while the blades continued to rotate at 25 rpm. The time that the torque reached a steady level was designated as ''time equal to zero.'' This premixed material was then subjected to an additional 5, 20, and 40 min of mixing at 25 rpm in the torque rheometer/batch mixer to generate specimens which are designated as ''specimens batch mixed for 5, 25, and 45 min.'' The mixtures were sealed into ointment jars, which were kept in a refrigerator at 4°C to prevent the evaporation of water content of the binder. These specimens were then compression molded under vacuum to provide the specimens for the characterization of their degree of mixedness using WAXD. Molded samples were dried in air and polished to

smooth the imperfections caused by contraction of material during drying.

Twin-Screw Extrusion

Basic Design of the MPR 7.5-mm Twin-Screw Extruder. The MPR 7.5-mm twin-screw extruder [5–7] shown in Figs. 4 and 5 was used (overall view, the screws used and the barrel halved opened to reveal the twin screw in Fig. 4 and the screws upon a dead stop during processing to reveal the degree of fill distribution in the mixer in Fig. 5). Some of the critical dimensions of the extruder include: the bore diameter is 7.5 mm and the screw diameter is 7.38 mm, the centerline distance between screws is 6.27 mm, the root diameter of the screw is 5.04 mm, and the tolerance on the screw diameter is $\pm$ 60 µm. The fully intermeshing co-rotating twin-screw extruder is designed with a slit die as an integral part of the assembly (Fig. 4). The dimensions of the die are: width of 10 mm, gap of 1 mm, and length of 50.8 mm, including 14 mm axial length for the converging flow section and 36.8 mm for the straight land section.

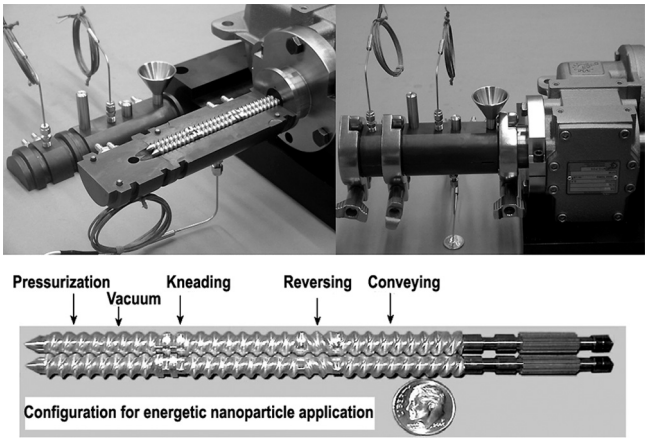

Figure 4. Twin-screw extruder specifically designed and built for incorporating nanoparticles.

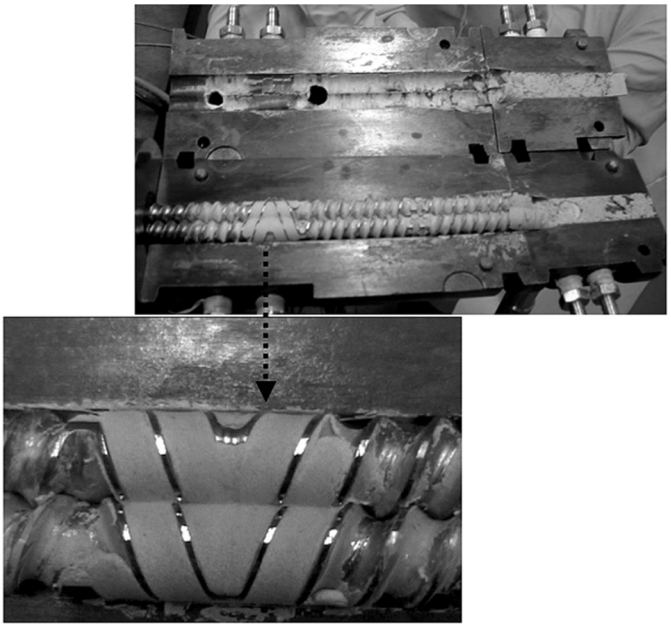

Figure 5. The typical degree of fill distributions in the twin-screw extruder upon a dead stop.

The assembly included three temperature control zones, one at the die and two at the extruder barrels. The machine is fitted with three thermocouples for controlling the metal temperature of the top and bottom barrel halves and the die assembly. The screw speed is controllable between 0 rpm and 200 rpm. The barrels and screws are machined from a heat-treated alloy stainless steel and ferritic nitro carburized to reduce the potential of adhesive wear between the screws and the barrel bores. The drive is a 1/4-HP motor, hydrostatic, 0–1100 rpm, 100% explosion proof. This is coupled through a parallel shaft speed reducer, 11.66:1 reduction ratio to give us a screw speed of 200 rpm when taking into account the speed increase, 2.166 to 1, through the ring and pinion gear set on the agitator shafts.

The screw configuration was designed through mathematical modeling of the mixer/extruder and die (using three-dimensional

finite element method). The screws are monolithic (Fig. 4); that is, they are constructed from a solid piece of bar stock with no welds, joints, cracks, or crevices for material to migrate into. The screw design consists of three sealed mixing and vacuum zones, as shown in Fig. 4. The fully flighted conveying/plasticization section (Section I) is sealed with a reverse fully flighted element. As shown with mathematical modeling, the screw elements need to be completely full to be able to generate the pressure necessary to force the binder of the suspension to go through the reversely configured section, which follows the forwarding elements. As shown in Fig. 5, this is indeed what was revealed when the extruder was brought to a dead stop and the distribution of the material in the extruder was investigated. The mixing zone for the incorporation of the nanoparticles into the hydrogel (Section II) is sealed with four pairs of 90° kneading discs. The screw is also expected to be completely full at the second kneading disc section and immediately preceding the set of kneading blocks (Fig. 5) and at the fully flighted section preceding the die. These were again the locations that experiments revealed to be completely full as expected, as shown in Fig. 5. The imposition of vacuum and consequent devolatilization takes place in the section between the kneading disks and the die (Section III).

Data Acquisition and Control

A PC-based and field point capable data acquisition and process control system was used (Fig. 6). The system is a state-of-the-art open architecture PC-based system and includes the instruments to monitor and control zone temperatures, product temperature, process pressure, and screw speed. The employed field point technology allows the data to be accessible remotely and the extruder to be run remotely (turn on, off, set the screw speed, set the temperatures of the oil circulating) using the remote Internet connections and also wireless.

There is one explosion-proof pressure transducer and thermocouple combination at the converging section of the die inlet. There is one temperature control thermocouple in the die

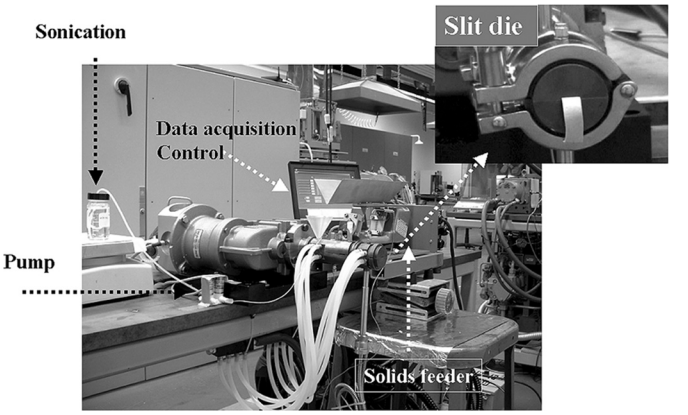

Figure 6. The auxiliaries of the twin-screw extruder specifically designed and built for incorporating nanoparticles.

assembly. Two temperature control thermocouples are placed in the barrel, one in the upper and one in the lower half. Temperature control is achieved through the circulation of heat transfer medium at desired temperature. An intrinsically safe tachometer pickup is located at the coupling to the parallel shaft reducer to monitor screw speed.

Feeding of the Ingredients. A number of options were tested for the feeding of the ingredients. The nanoparticles arrived in a water medium since they were completely oxidized. The CMC was initially in powder form. The loss in weight and volumetric feeders of K-Tron and Brabender (integrated to the MPR control system, Fig. 6) were tested. The Brabender and the K-Tron units generated acceptable feed rate results. A miniaturized pump was used for the feeding of the nanoparticles in a water carrier (Fig. 6).

Twin-Screw Extrusion Processing Runs. The pressure data were collected to determine the pressure drop at the die. The temperature of the material could be followed with the thermocouples as verified with the thermal imaging camera,

which was incorporated into the experimental setup. Such thermal images were collected at regular intervals to allow the following of the temperature history of the extrudate. The binder content values of the extrudates were also determined to assure that the binder could be conserved in the extruder.

Rheological Characterization

Dynamic Properties. The small-amplitude oscillatory shear flow was used for the characterization of the linear viscoelastic properties of the suspension samples as a function of time, strain, and frequency. The Advanced Rheological Extended System (ARES) of Rheometric Scientific (currently TA Instruments) was used in conjunction with the 8-mm parallel disk fixtures for the small-amplitude oscillatory shear experiments. Considering that the gap between the plates was typically kept at 1 mm, the quantity of the suspension probed during the small-amplitude oscillatory shear experiments was around 70 mg.

Degree of Mixedness Analysis (Statistics of Concentration Distributions). The following analysis was used to characterize the statistics of the concentration distributions to provide a measure of the degree of mixedness or mixing indices of the graphite and the binder. If N measurements of the concentration, c_i, of one of the ingredients of the formulation are made, then the mean, $\bar{c}$, and the variance, s^2, of the concentration distribution of this ingredient are calculated from:

$$\bar{c} = \frac{1}{N}\sum_{i=1}^{N} c_i \tag{2}$$

$$s^2 = \frac{1}{(N-1)}\sum_{i=1}^{N} (c_i - \bar{c})^2 \tag{3}$$

The difference between the mean concentration, $\bar{c}$ and the known overall concentration, ϕ, of an ingredient (minor or the major component) is indicative of the quality of the

sampling technique [1,2,8–10]. This difference between $\bar{c}$ and ϕ diminishes as the number, N, of the characterized samples increases. The measured concentration values of a component of the mixture depend also on the sample size [8–13]. These concentration values approach the overall concentration of the component in the mixture, ϕ, as the sample size or the scale of the examination is increased. On the other hand, as the scale of the examination is reduced, the concentrations of the ingredients would deviate significantly from their mean values and in the limit the variance of the concentrations measured would reach the variance of a segregated sample [8].

The variance, s^2, arising from the distributions of the individual concentration values, i.e., c_i measurements, provides the most basic measure of the concentration homogeneity of a mixture [11]. Thus, the determination of the statistics of the extent to which the concentration values at various regions of the volume of the mixture differ from the mean concentration can be used as an index to quantitatively assess the degree of mixedness [12,13].

A small variance value would suggest that the mixture approaches the behavior of a homogeneous system, where most of the samples yield c_i values that are approaching $\bar{c}$. On the other hand, if the components of a mixture are completely segregated, the maximum variance occurs. The value of the maximum variance (or the square of the between-sample standard deviation) for a completely segregated system can be defined by assuming that the samples are taken from either one component or the other without crossing a boundary [12,13]:

$$s_0^2 = \bar{c}(1 - \bar{c}) \tag{4}$$

On the other hand, the most ideal state of random mixing possible would be achieved when the variance of the concentrations of the targeted ingredient sampled from different locations in the mixture would reach the variance of the binomial distribution. The variance for the binomial distribution is given as [11,12]:

$$s_r^2 = \frac{\overline{c}(1 - \overline{c})}{n} \tag{5}$$

where s_r^2 is the variance of a random mixture determined on the basis of the binomial distribution and n is the number of particles in the sample, with each particle belonging to either the minor or the major component. As the number of particles in a mixture, n, increases, the variance of the binomial distribution would approach zero.

The variance of the distribution of the concentrations of a given ingredient can be normalized with its maximum value and the resulting parameter provides a measure of the degree of mixedness; i.e., one possible mixing index for that particular ingredient. This parameter, s^2/s_0^2, would be equal to one for completely segregated ingredients and would decrease toward zero as the homogeneity of the mixture improves. Other definitions of mixing indices can be derived from the concentration distributions, the mean composition, the sample weight, and the particle size distributions of the components [12]. Various factors might affect the calculated mixing indices. For example, the mixing indices show an increase with a decrease in the amount of the minor phase [12]. Sample size [8,12] and the number of samples analyzed also affect the values of the mixing indices.

For this study the following measure of the degree of mixedness, i.e., mixing index, which is based on the standard deviation of the distribution of the concentration of one of the ingredients of the formulation over the standard deviation of the completely segregated sample for the same ingredient, was used. This mixing index would exhibit a value of zero for a completely segregated sample and its value would approach one for a completely random distribution of the concentrations of its ingredients.

$$\text{Mixing Index} = 1 - \frac{s}{s_0} \tag{6}$$

Wide-Angle X-Ray Diffraction (WAXD). Diffraction patterns can be analyzed quantitatively, because the intensity from a particular phase in a mixture of phases depends on the concentration of that phase in the mixture. However, the relation between the integrated intensity I_x and the volume

fraction ϕ_x of a phase is nonlinear, because the diffracted intensity depends strongly on the absorption coefficient of the mixture, μ_m, which itself depends on the concentration. For a two-phase material (with absorption coefficients μ_1 and μ_2 for the individual phases), the absorption coefficient for the mixture becomes [1,2,8–10]:

$$\mu_m = \phi_1\mu_1 + \phi_2\mu_2 \tag{7}$$

The integrated intensity from phase 1 is then given by:

$$I_1 = K_1\phi_1/\mu_m \tag{8}$$

where K_1 is a constant that depends on the material and the incident beam used but not on the concentration. The ratio of intensities from phases 1 and 2, however, is independent of μ_m and varies linearly with concentration [8]:

$$I_1/I_2 = (K_1/K_2)\phi_1/\phi_2 \tag{9}$$

The intensity values associated with the amorphous phase and the nanoparticles were normalized with the total intensity values and the variance values of these ratios were obtained. These variance values are equivalent to the variances of the distributions of the concentrations of the amorphous binder phase and nanoparticles, respectively.

A Rotaflex (rotating anode) RTP300RC X-ray diffractometer by Rigaku was used for small beam–size scans at a fixed voltage of 40 kV and current of 80 mA. Samples were run at a scanning speed of 0.5° per min, using a sampling width of 0.02°, and within the Bragg angle, 2θ, range of 13–50°. The X-ray probe had 1.5 mm diameter (1.18 mm^2) at a Bragg angle, 2θ, of 90°.

Typical X-ray diffraction pattern of the composite, i.e., the typical intensity versus the Bragg angle data, is shown in Fig. 7. The deconvolution of the diffraction pattern to separate the contributions of its ingredients was made possible upon the identifications of the peaks, which are associated with the pure ingredients; i.e., the alumina nanoparticles and the CMC hydrogel binder, as shown in Fig. 7. The area under a particular

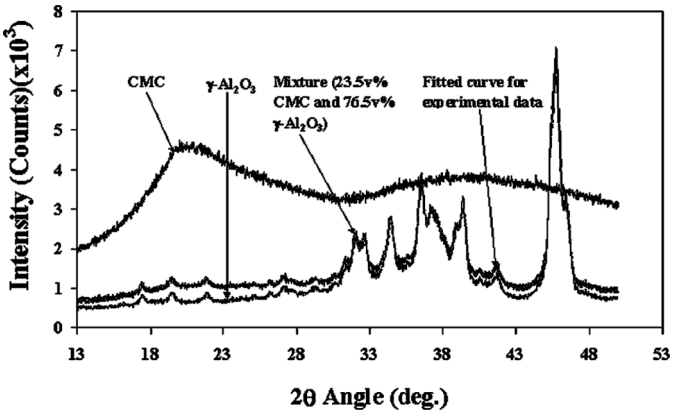

Figure 7. Typical X-ray diffraction patterns of the simulant formulation and its various ingredients.

crystalline peak of γ-Al_2O_3 could be used to represent the γ-Al_2O_3 intensity, $I_{\gamma\text{-}Al_2O3}$. In another method, instead of the use of a single peak that is characteristic of each phase, all peaks associated with the particular phase were used in the analysis. Upon the subtraction of the peaks arising from γ-Al_2O_3, the contribution of the amorphous phase (NaCMC) was determined from the signal of the composite mixture between the Bragg angles of 13 to 50° (Fig. 7). This contribution of the amorphous phase (the binder phase) is designated with the intensity, I_{Amorph}. The mixing indices were calculated on the basis of the variance values of the ratio of the intensity of the γ-Al_2O_3 and the intensity of the amorphous over the total intensity; i.e., $I_{\gamma\text{-}Al_2O3}/I_T$ or I_{Amorph}/I_T, respectively.

Thermo-Gravimetric Analysis (TGA). A TA Instruments thermo-gravimetric analyzer, Q50, was used for the characterization of the decomposition of the individual components and the mixtures as a function of temperature. The thermo-gravimetric analyzer measures the rate of weight change of a specimen as a function of increasing temperature under a controlled inert gas environment. In TGA the sample size was around 2 mg.

Each specimen was scanned from ambient to 700°C with a heating rate of 15°C/min (Fig. 8). Individual runs with just the CMC and the nanoparticles separately were also carried out. TGA and DSC analysis of pure CMC revealed that the CMC loses its moisture around 100°C and it starts decomposing partially around 215°C. Decomposition continues at decreasing rates until 700°C. However, CMC does not completely decompose and leaves a residue of about 33–34%.

The CMC concentration for different mixture samples could be determined by using a calibration curve. To be able to generate the calibration curve, three different mixtures with CMC volume fractions of 0.25, 0.27, and 0.29 (as measured in dry samples; i.e., upon the removal of the water from the mixture) were used. These samples with known concentrations were run under the same conditions in the temperature range between 25 and 700°C. During calibration runs, the sample sizes were kept constant at around 50 mg to generate a sufficiently large scale of examination to approach the mean concentration of the samples. TGA and DSC analysis of pure nano γ-Al_2O_3 indicated that the nano γ-Al_2O_3 only loses its moisture around 100°C and this amount (depending on the relative

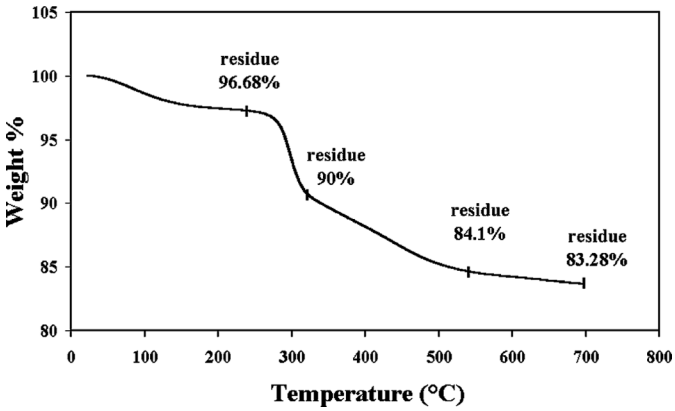

Figure 8. Typical thermo-gravimetric analysis results of the simulant formulation.

humidity of the environment) changes between 1 to 2%. Mixing indices were also calculated from the results of the thermogravimetric analysis experiments by following Eqs. (2)–(6) and were compared with the mixing indices obtained with wide-angle X-ray diffraction.

Results and Discussion

Rheology

The typical small-amplitude oscillatory shear behavior of the suspensions (with γ-Al_2O_3) is shown in Figs. 9 and 10. The storage, G', loss modulus, G'', and the magnitude of complex viscosity, $|\eta^*|$, values of the suspension samples prepared with the twin-screw extrusion process are significantly smaller than those processed with the conventional intensive batch processing method. Generally the reductions of the elasticity and the shear viscosity of a suspension occur when better distribution and dispersion of the phases are achieved (better concentration homogeneity and a reduction of the particle agglomerates) [14–16].

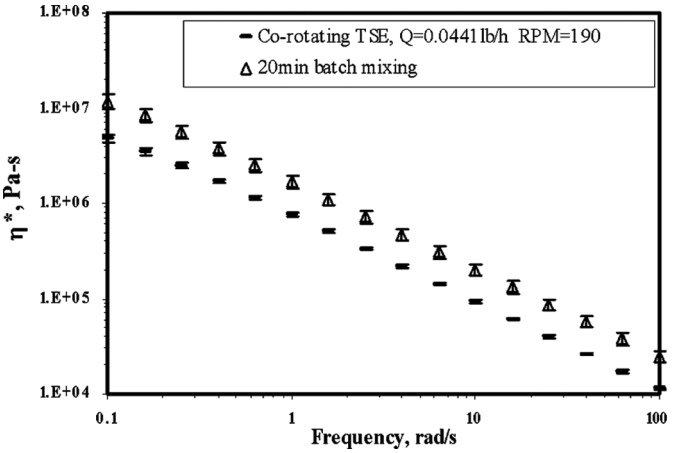

Figure 9. Confidence intervals of the magnitude of complex viscosity data for mixtures prepared with conventional and twin-screw extrusion processes.

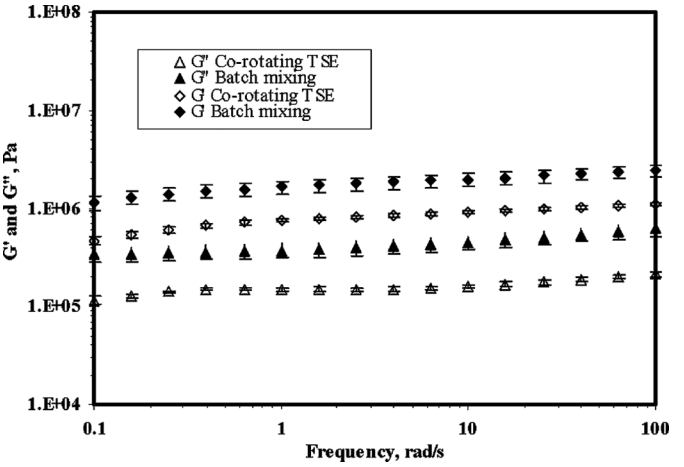

Figure 10. Confidence intervals of the storage modulus, G′, and loss modulus, G″, data for mixtures prepared with conventional and twin screw extrusion processes.

Degree of Mixedness Analysis

The distributions of the ratios of the intensities arising from the gamma alumina nanoparticles over the total intensity obtained with the wide angle X-ray diffraction method are shown in Fig. 11. The broader the variation of the intensity ratios around the mean, the poorer is the homogeneity of the concentrations of the gamma alumina nanoparticles versus the gel binder. According to these WAXD results, in line with the results of dynamic properties, a narrower distribution of the concentration of γ-Al_2O_3 could be obtained with the twin-screw extrusion process in comparison to the batch mixing process. The distributions of the concentration of alumina nanoparticles in the binder as obtained with the TGA method are shown in Fig. 12. TGA results also validate the findings of the X-ray method by indicating that the variation of the concentrations of γ-Al_2O_3 is much broader upon batch mixing (suggesting a poorer state of homogeneity of the γ-Al_2O_3 nanoparticles upon batch mixing) than twin-screw extrusion.

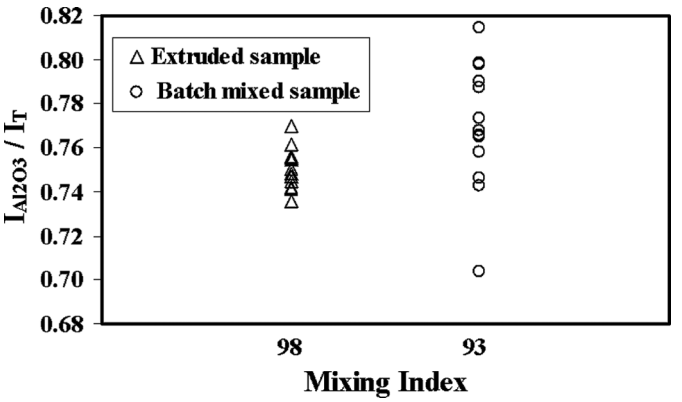

Figure 11. Scatter of the X-ray diffraction data for mixtures prepared with conventional and twin-screw extrusion processes and their mixing indices.

From WAXD the mixing index value of γ-Al_2O_3 nanoparticles in the hydrogel binder is 0.98 for the twin-screw extrusion product versus 0.93 for batch (1 represents a perfectly homogeneous mixture and 0 represents a segregated sample with no intermixing of the ingredients), as shown in Fig. 11. From TGA the mixing index values for γ-Al_2O_3 are 0.9 for the batch-mixed samples and 0.95 for the twin-screw–extruded samples (Fig. 12). Overall, the higher values of the mixing indices for the twin-screw extrusion process again indicate that better distributive mixing of the nano-alumina could be achieved with the twin-screw extrusion process than batch mixing. These findings obtained with thermo-gravimetric analysis and wide-angle X-ray diffraction were verified using scanning and transmission electron microscopy and polarized microscopy, which enabled the collection of data on the size of the particle clusters/agglomerates generated during batch mixing and twin-screw extrusion.

Microscopy

Overall, the better distribution and smaller agglomerate sizes of the γ-Al_2O_3 suspensions processed with twin-screw extrusion

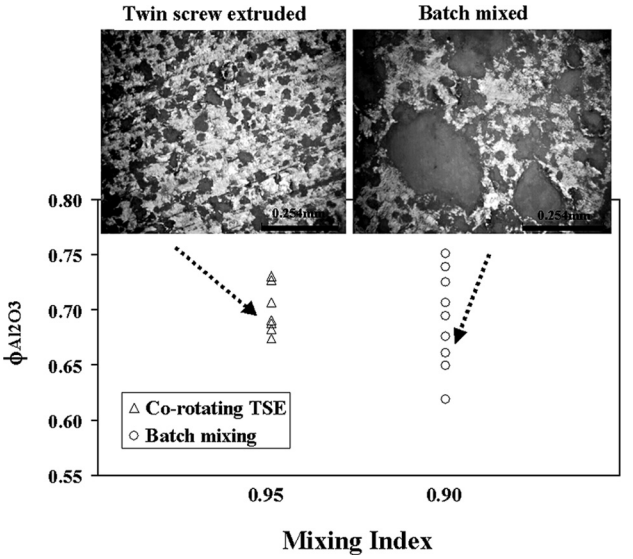

Figure 12. Scatter of the thermo-gravimetric analysis data for mixtures prepared with conventional and twin-screw extrusion processes and their mixing indices.

could be clearly seen under polarized microscopy as shown in Fig. 12. The much better distribution of the phases upon twin-screw extrusion is clearly indicated upon the comparisons of the micrographs of twin-screw–extruded and batch-mixed samples shown in Fig. 12.

The microscopy, the WAXD and TGA results indicate that in spite of the much better homogeneity of the nanoparticles achieved with twin-screw extrusion, nano-alumina particles largely remained as clusters/agglomerates (at reduced domain sizes upon twin-screw extrusion). This is clearly shown in the typical SEM micrograph in Fig. 13 and TEM micrographs given in Figs. 14 and 15. Both the alpha and gamma alumina nanoparticles appear as clusters, not coated individually by the binder, and clearly identified interfaces are developed between the nanoparticle clusters and the CMC binder. The typical TEM micrographs shown in Figs. 14 and 15 clearly

indicate that some of the nanoparticles form agglomerates that have significantly reduced surface-to-volume ratios in comparison to those of the individual nanoparticles.

These results pinpoint the main challenge associated with the compounding of nanoparticles into various energetic formulations; i.e., the generation of agglomerates that cannot be broken down. Using a CL-20–based formulation, Greenberg et al. [3,4] have shown that efficiency of the coating of energetic particles with the binder is critical in the control of important ultimate properties, including the sensitivity of energetic formulations. Although twin-screw extrusion does help in better distribution and dispersion of the nanoparticle agglomerates and reducing the size of the agglomerates, the proper tailoring of the binder and surfactants, to enable the wetting of the nanoparticle surfaces properly and thus separate them from each other, appears to be the critical factor in the compounding of nanoparticles into energetic formulations. This is elaborated next.

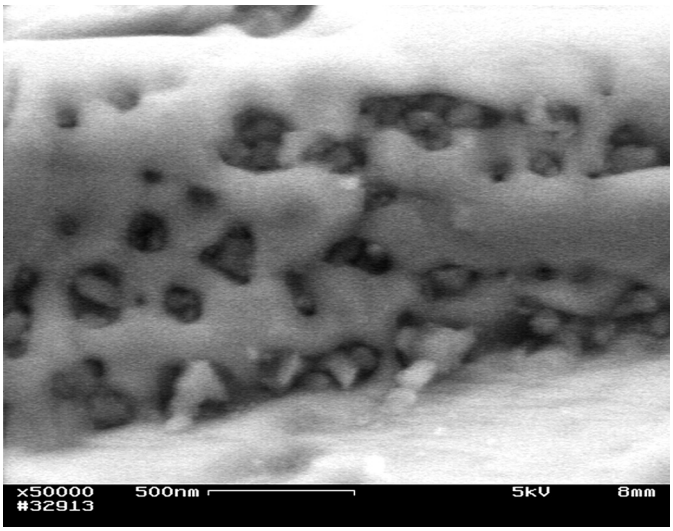

Figure 13. Typical SEM micrograph of batch-mixed samples.

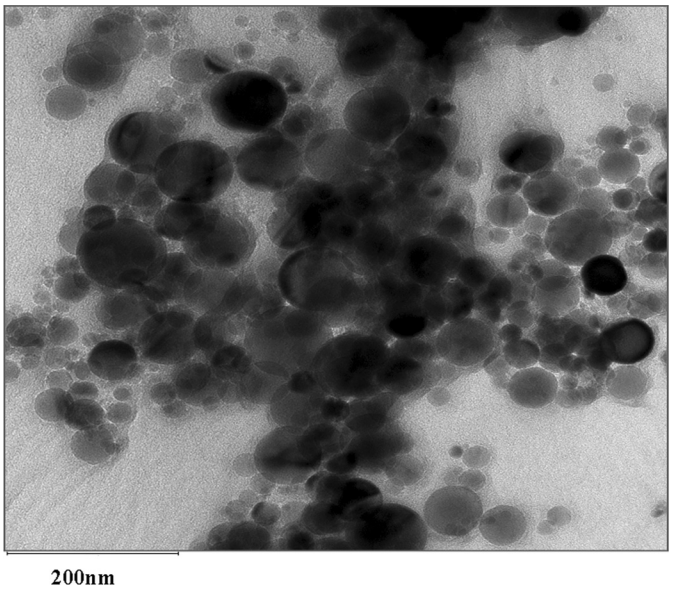

Figure 14. Typical TEM micrograph showing nanoparticle clusters.

The Use of Surfactants to Better Disperse the Nanoparticles

To improve dispersion we have tried one surfactant each for the targeted better wetting of the alpha and gamma nanoparticles with the binder (surfactant used at 0.125% by weight of the nanoparticles or 0.08% by weight of the total dry weight). Some of the rheological characterization results of the surfactant-containing suspensions of the nanoparticles upon both batch mixing and twin-screw extrusion are shown in Fig. 16. According to these results, the surfactant used for the wetting of the gamma alumina nanoparticles (i.e., ammonium polyacrylate, with trade name Darvan 821 A, procured from R.T. Vanderbilt Company, Norwalk, CT) was not effective in batch mixing but showed some effectiveness upon twin-screw extrusion. On the other hand, the surfactant used for the wetting of the alpha nanoparticles (ammonium polymethacrylate, with

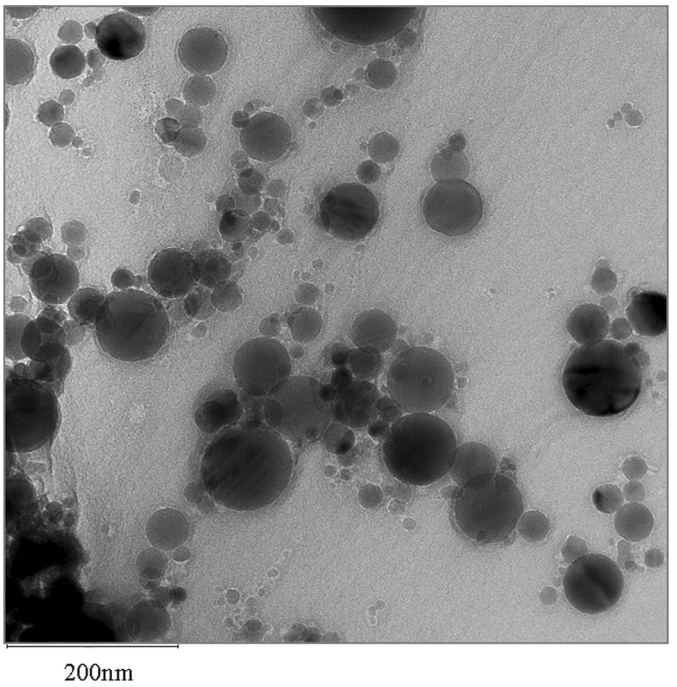

Figure 15. Typical TEM micrograph showing better dispersion of nanoparticles.

trade name Darvan C, which was selected on the basis of molecular modeling and procured from Vanderbilt) was found to be more effective. This is clearly seen from the typical results given in Fig. 16, which indicate that the use of the ammonium poly methacrylate surfactant for the alpha nanoparticles gave rise to a clear reduction in the elasticity, i.e., G', the energy dissipated as heat upon one cycle of deformation, i.e., loss modulus, G'', and the viscosity of the suspensions for both the batch-mixed and twin-screw extruded samples.

Overall, upon the incorporation of the surfactants, the twin-screw extrusion process again generates the lowest elasticity and viscosity for both the alpha alumina and gamma alumina nanoparticles, suggesting again better mixing and dispersion of the nanoparticles and the reduction of the

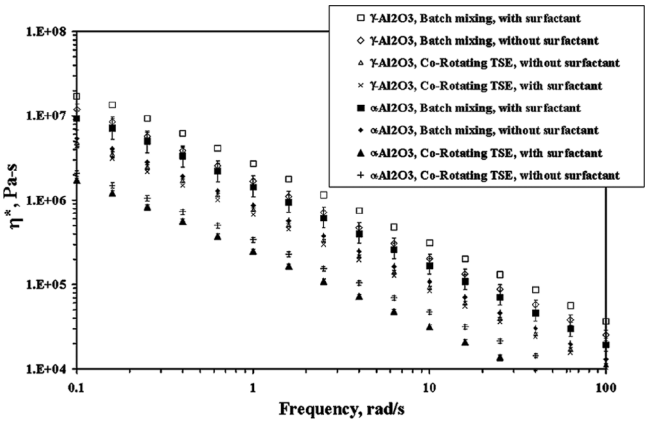

Figure 16. Typical magnitude of complex viscosity versus frequency data for suspensions prepared with or without the use of surfactants and processed with twin-screw extrusion or conventional batch processing.

nanoparticle cluster domains could be obtained upon twin-screw extrusion than batch mixing.

Conclusions

This study has demonstrated some of the challenges associated with the dispersion of nanoparticles in energetic formulations. The conclusions are summarized as:

1. The incorporation of nanoparticles into gel-like binders commonly used in various energetic formulations has been explored using a novel twin-screw extruder specifically designed and built to handle nanoparticles and energetic materials at relatively low flow rates.
2. The twin-screw extrusion process is shown to have various inherent advantages including the small size of the processed material within the confines of the processor at any given time, the ability to remove the air content during the process, the ability to shape the formulation as part of the process, the higher surface-to-volume ratio

to give rise to better temperature control, and the better dispersion of the nanoparticles in the binder matrix.

3. However, the adequate dispersion of the nanoparticles in energetic formulations is not a simple task regardless of which process is used, if the formulation does not allow for the proper wetting of the nanoparticles by the binder. If the binder and the surfactants are not selected properly, the nanoparticles remain as agglomerates. The sizes of the agglomerate can be reduced, but such agglomeration of the nanoparticles is not likely to be completely eliminated on the basis of the use of the twin-screw extrusion technology alone without the benefit of proper selection of the binder and the surfactants to control the interfacial properties between the binder and the nanoparticles.
4. The use of surfactants has been successfully demonstrated to enable better dispersion of the nanoparticles and reduction of the size of agglomerates of nanoparticles.
5. The availability of this novel mini twin-screw extruder should enable for the first time the testing of binders and surfactants at relatively small scales but under industrially-relevant processing conditions (aiming to generate realistic mixtures that can be scaled up into manufacturing scale).
6. The task of development of formulations can be significantly improved since the mini extruder eliminates the need to mix ingredients by hand or using batch mixers.

Acknowledgements

Financial support of Picatinny TACOM under contract DAAE30-02-BAA-0800 and the contributions of B. Reddingius are gratefully acknowledged. The TEM analysis was carried out at Penn State University under the leadership of Dr. G. Nang. The surfactants used in the study were suggested by Dr. H. Gocmez.

References

[1] Yazici, R. and D. M. Kalyon. 1996. Quantitative characterization of degree of mixedness of LOVA grains. *Journal of Energetic Materials*, 14(1): 57–73.

[2] Yazici, R., D. Kalyon. and D. Fair. 1998. Microstructure and Mixing Distribution Analysis in M30 Triple-base Propellants. Report #ARWEC-CR-98015, U.S. Army Armament Research, Development and Engineering Center, Warheads, Energetics and Combat Support Armaments Center, Picatinny Arsenal, NJ.

[3] Greenberg, B. L., D. M. Kalyon, M. Erol, M. Mezger, K. Lee, and S. Lusk. 2003. Analysis of slurry-coating effectiveness of CL-20 using a novel grazing incidence X-ray diffraction method. *Journal of Energetic Materials*, 21(1): 185.

[4] Greenberg, B., D. Kalyon, M. Erol, M. Mezger, P. Redner, K. Lee, and S. Lusk. 2003. Structural Analysis of Slurry Coated CL-20 (PAX 12 Granules) Using a Novel Grazing Incidence X-Ray Diffraction Method. Proceedings of Joint Army, Navy, NASA, Air Force Propellant Development and Characterization Meeting, Charlottesville, VA, March 26.

[5] Kowalczyk, J. E., J. B. Graybill, M. Malik, D. Kalyon, H. Gevgilili, M. Mezger, and B. Reddingius. 2004. Novel Extrusion Platforms for the Continuous Processing of Energetics. AICHE Annual Meeting, Austin, Texas, November 11.

[6] Kowalczyk, J., J. Graybill, B. Karuv, D. Kalyon, H. Gevgilili, M. Zghaibeh, S. Ozkan, M. Mezger, and B. Reddingius, 2004. Design and Manufacture of the Smallest Twin Screw Extruder in the World for the Processing of Nanoparticles into Nanoenergetics and Nanocomposites. Proceedings of the 13th Joint Ordnance Commanders Group (JOCG) Continuous Mixer and Extruder Users Group Meeting. Hoboken, NJ, October 14.

[7] Materials Processing & Research, Inc. http://www.mprus.com <accessed November 10, 2006>.

[8] Yazici, R. and D. M. Kalyon. 1993. Degree of mixing analyses of concentrated suspensions by electron probe and X-ray diffraction. *Rubber Chemistry and Technology*, 66(4): 527–537.

[9] Yazici, R. and D. M. Kalyon. 1998. Quantitative Measurement of Mixing Quality. Proceedings of 1998 Joint Army, Navy, NASA, Air Force Propellant Development and Characterization Meeting, Houston, TX, April 20–24.

[10] Yazici, R., D. Kalyon, and D. Fair. 1998. Microstructure and Mixing Distribution Analysis in M30 Triple-Base Propellants. ARDEC Information Research Center ARWEC CR 98015, Picatinny Arsenal, NJ, September 15.
[11] Tadmor, Z. and C. G. Gogos. 1979. *Principles of Polymer Processing*. New York: John Wiley.
[12] Schofield, C. 1976. The definition and assessment of mixture quality in mixtures of particulate solids. *Powder Technology*, 15: 169.
[13] McKelvey, J. M. 1962. *Polymer Processing*. New York: John Wiley.
[14] Kalyon, D., E. Birinci, R. Yazici, B. Karuv, and S. Walsh. 2002. Electrical properties of composites as affected by the degree of mixedness of the conductive filler in the polymer matrix. *Polymer Engineering & Science*, 42(7): 1609–1617.
[15] Erol, M. and D. Kalyon. 2005. Assessment of the degree of mixedness of filled polymers: Effects of processing histories in batch mixer and co-rotating and counter-rotating twin screw extruders. *International Polymer Processing*, 20: 228–237.
[16] Kalyon, D., D. Dalwadi, M. Erol, E. Birinci, and C. Tsenoglu. 2006. Rheological behavior of concentrated suspensions as affected by the dynamics of the mixing process. *Rheologica Acta*, 45: 641–658.